

Numerical Solution of Multi-Order Fractional Differential Equations Using Generalized Sine-Cosine Wavelets

Somayeh Nemati^{a*} and Anas Al-Haboobi^a

^aDepartment of Mathematics, Faculty of Mathematical Sciences, University of Mazandaran, Babolsar, Iran

*Corresponding author

Article Info

Keywords: Block-pulse functions, Generalized sine-cosine wavelet, Multi-order fractional differential equations, Operational matrix of fractional integration

2010 AMS: 26A33, 65N35, 65T60,

Received: 26 May 2018

Accepted: 26 September 2018

Available online: 20 December 2018

Abstract

In this work, we propose a numerical method based on the generalized sine-cosine wavelets for solving multi-order fractional differential equations. After introducing generalized sine-cosine wavelets, the operational matrix of Riemann-Liouville fractional integration is constructed using the properties of the block-pulse functions. The fractional derivative in the problem is considered in the Caputo sense. This method reduces the considered problem to the problem of solving a system of nonlinear algebraic equations. Finally, some examples are included to demonstrate the applicability of the new approach.

1. Introduction

The notion of the fractional differential equations (FDEs) was first developed as a pure mathematical theory in the middle of the 19th century [1]. A history of the development of the fractional differential operators can be found in [2, 3]. It has been revealed that many mathematical modelings contain FDEs. To mention a few, fractional derivatives are used in viscoelastic systems [4], economics [5], continuum and statistical mechanics [6], solid mechanics [7], electrochemistry [8], biology [9] and acoustics [10]. An important issue to shed light on is the fact that most of the FDEs do not have exact analytic solutions. Consequently, emphasis of efforts is on the importance of seeking numerical solutions for these equations. As a result, several numerical methods have been given to solve problems including FDEs, such as Adomian decomposition method [11], variational iteration method [12], fractional differential transform method [13], operational matrix method [14], homotopy analysis method [15], power series method [16] and modified homotopy perturbation method [17]. Also, there can be some classical solution techniques to be found, e.g. Laplace transform method [18].

One way to solve equations numerically is to use wavelets. The basic idea of wavelets (both: translation and dilation) goes back to the early 1960's [19]. There are developments concerning the multiresolution analysis (MRA) algorithm based on wavelets [20] and the construction of compactly supported orthonormal wavelet bases [21]. Wavelets constitute unconditional (Riesz) bases for $L^2(\mathbb{R})$, the space of all square integrable functions on the real line. In other words, a function in $L^2(\mathbb{R})$ can be decomposed and stably reconstructed in terms of wavelets [22]. To illustrate, some wavelets which have been constructed and used for solving FDEs include B-spline wavelets [23], Haar wavelets [24], Chebyshev wavelets [25], Legendre wavelets [26] and Bernoulli wavelets [27].

Sine-cosine wavelet (SCW) has been used and showed efficient to solve various problems. To indicate this, we can refer to some works. Razzaghi and Yousefi in [28] have employed SCW to solve variational problems. Tavassoli Kajani et al. [29] have proposed a method based on SCW for solving integro-differential equations. They also applied this method to solve Fredholm integral equations in [30]. A numerical evaluation of Hankel transform for seismology has been given in [31] using SCWs approach. The present work introduces the generalized sine-cosine wavelets (GSCWs) operational matrix of fractional integration which can be used to solve fractional problems.

The organization of this paper is as follows: Section 2 gives a brief preliminaries of fractional calculus followed by orthonormal basis of GSCWs and their properties in Section 3. Section 4 is devoted to block-pulse functions and their basic properties. Section 5 introduces the fractional order of operational matrix of integration for GSCWs. A numerical method based on the GSCWs and block-pulse functions in order to solve multi-order FDEs is given in Section 6. Some examples are included in Section 7 to show the applicability and efficiency of this method followed by concluding remarks in Section 8.

2. Preliminaries of fractional calculus

In this section, we briefly give some preliminaries and notations of fractional calculus. Two most important definitions for fractional integral and derivative operators are Riemann-Liouville integral and Caputo derivative. The Riemann-Liouville fractional integral operator I^α of order $\alpha \geq 0$ is defined as follows [32]:

$$I^\alpha u(t) = \begin{cases} \frac{1}{\Gamma(\alpha)} \int_0^t (t-s)^{\alpha-1} u(s) ds, & \alpha > 0, \\ u(t), & \alpha = 0, \end{cases}$$

where $\Gamma(\alpha)$ is the gamma function defined by

$$\Gamma(\alpha) = \int_0^\infty t^{\alpha-1} e^{-t} dt.$$

Also, the Caputo fractional derivative operator D^α of order α is defined as follows [32]:

$$D^\alpha u(t) = \frac{1}{\Gamma(n-\alpha)} \int_0^t (t-s)^{n-\alpha-1} u^{(n)}(s) ds, \quad n-1 < \alpha \leq n, \quad n \in \mathbb{N},$$

where $n = \lceil \alpha \rceil$ is the smallest integer greater than or equal to α .

The following properties are satisfied for the Riemann-Liouville integral operator and Caputo derivative:

$$I^\alpha t^v = \frac{\Gamma(v+1)}{\Gamma(v+1+\alpha)} t^{v+\alpha}, \quad v > -1,$$

$$I^\alpha (D^\alpha u(t)) = u(t) - \sum_{i=0}^{\lceil \alpha \rceil - 1} u^{(i)}(0) \frac{t^i}{i!}, \quad (2.1)$$

$$I^{\alpha-\beta} (D^\alpha u(t)) = D^\beta u(t) - \sum_{i=\lceil \beta \rceil}^{\lceil \alpha \rceil - 1} u^{(i)}(0) \frac{t^{i-\beta}}{\Gamma(i-\beta+1)}, \quad 0 \leq \beta < \alpha. \quad (2.2)$$

3. Generalized sine-cosine wavelets

3.1. Definition and function approximation

Wavelets constitute a family of functions constructed from dilation and translation of a single function $\varphi(t)$ which is called the mother wavelet. When the dilation parameter and the translation parameter vary continuously, we have the following family of continuous wavelets as [19, 33, 34]

$$\Psi_{a,b}(t) = |a|^{-\frac{1}{2}} \varphi\left(\frac{t-b}{a}\right), \quad a, b \in \mathbb{R}, \quad a \neq 0,$$

where a and b are the dilation and translation parameters, respectively. If the parameters a and b are restricted to take values $a = a_0^{-k}$ and $b = nb_0 a_0^{-k}$, where $a_0 > 1$, $b_0 > 0$ and n , and k are positive integers, a family of discrete wavelets which forms a wavelet basis for $L^2(\mathbb{R})$ is obtained as

$$\Psi_{k,n}(t) = |a_0|^{\frac{k}{2}} \varphi\left(a_0^k t - nb_0\right).$$

Especially, if $a_0 = 2$ and $b_0 = 1$, then the set $\{\Psi_{k,n}(t)\}$ forms an orthonormal basis.

SCWs are usually defined on the interval $[0, 1)$. Here, we replace the interval $[0, 1)$ by $[0, T)$ where $T > 0$ and define GSCWs as

$$\Psi_{n,m}(t) = \begin{cases} \frac{2^{\frac{k+1}{2}}}{\sqrt{T}} f_m(2^k t - nT), & \frac{n}{2^k} T \leq t < \frac{n+1}{2^k} T, \\ 0, & \text{otherwise,} \end{cases}$$

with

$$f_m(t) = \begin{cases} \frac{1}{\sqrt{2}}, & m = 0, \\ \cos\left(\frac{2m\pi t}{T}\right), & m = 1, 2, \dots, L, \\ \sin\left(\frac{2(m-L)\pi t}{T}\right), & m = L+1, L+2, \dots, 2L, \end{cases}$$

where L is any positive integer, $n = 0, 1, 2, \dots, 2^k - 1$ and $k = 0, 1, 2, \dots$. The set of GSCWs forms an orthonormal basis for the space $L^2[0, T)$. Therefore, a function $u(t)$ in this space may be expanded in a series of GSCWs as

$$u(t) = \sum_{m=0}^{\infty} \sum_{n=0}^{2^k-1} c_{n,m} \Psi_{n,m}(t), \quad (3.1)$$

where

$$c_{n,m} = \langle u(t), \Psi_{n,m}(t) \rangle = \int_0^T u(t) \Psi_{n,m}(t) dt,$$

in which $\langle \cdot, \cdot \rangle$ denotes the inner product. If the infinite series in (3.1) is truncated, then an approximation of the function $u(t)$ is obtained as

$$u(t) \simeq \sum_{m=0}^{2L} \sum_{n=0}^{2^k-1} c_{n,m} \Psi_{n,m}(t) = C^T \Psi_{\omega}(t), \tag{3.2}$$

where $\omega = 2^k(2L + 1)$, and C and $\Psi(t)$ are $2^k(2L + 1) \times 1$ matrices given by

$$C = [c_{0,0}, c_{0,1}, \dots, c_{0,2L}, c_{1,0}, c_{1,1}, \dots, c_{1,2L}, \dots, c_{2^k-1,0}, c_{2^k-1,1}, \dots, c_{2^k-1,2L}]^T,$$

$$\Psi_{\omega}(t) = [\Psi_{0,0}(t), \Psi_{0,1}(t), \dots, \Psi_{0,2L}(t), \Psi_{1,0}(t), \Psi_{1,1}(t), \dots, \Psi_{1,2L}(t), \dots, \Psi_{2^k-1,0}(t), \Psi_{2^k-1,1}(t), \dots, \Psi_{2^k-1,2L}(t)]^T.$$

3.2. Convergence analysis

In this section, we get the convergence of the GSCW approximation of a function for all level of resolution k .

Theorem 3.1. *Let $L \rightarrow \infty$, then the series solution (3.2) converges to $u(t)$.*

Proof. Let $S_{k,M}(t)$ be a sequence of partial sums of $c_{n,m} \Psi_{n,m}(t)$ as

$$S_{k,M}(t) = \sum_{m=0}^M \sum_{n=0}^{2^k-1} c_{n,m} \Psi_{n,m}(t),$$

where $M = 2L$. We prove that $S_{k,M}$ is a Cauchy sequence in Hilbert space $L^2[0, T]$ and then we show that $S_{k,M}$ converges to $u(t)$, when $M \rightarrow \infty$. In order to reach the first aim, let $\hat{M} = 2\hat{L}$ with $L > \hat{L}$, then

$$\begin{aligned} \|S_{k,M} - S_{k,\hat{M}}\|^2 &= \left\| \sum_{m=\hat{M}+1}^M \sum_{n=0}^{2^k-1} c_{n,m} \Psi_{n,m}(t) \right\|^2 \\ &= \left\langle \sum_{m=\hat{M}+1}^M \sum_{n=0}^{2^k-1} c_{n,m} \Psi_{n,m}(t), \sum_{m=\hat{M}+1}^M \sum_{n=0}^{2^k-1} c_{n,m} \Psi_{n,m}(t) \right\rangle \\ &= \sum_{m=\hat{M}+1}^M \sum_{n=0}^{2^k-1} \sum_{l=\hat{M}+1}^M \sum_{r=0}^{2^k-1} c_{n,m} c_{r,l} \langle \Psi_{n,m}(t), \Psi_{r,l}(t) \rangle \\ &= \sum_{m=\hat{M}+1}^M \sum_{n=0}^{2^k-1} |c_{n,m}|^2. \end{aligned}$$

From Bessel's inequality, we have $\sum_{m=0}^{\infty} \sum_{n=0}^{2^k-1} |c_{n,m}|^2$ is convergent. So

$$\|S_{k,M} - S_{k,\hat{M}}\|^2 \rightarrow 0 \text{ as } L \rightarrow \infty.$$

This suggests that $S_{k,M}$ is a Cauchy sequence and hence it converges to a function in $L^2[0, T]$, say, $f(t)$. We need to show that $f(t) = u(t)$,

$$\begin{aligned} \langle f(t) - u(t), \Psi_{n,m}(t) \rangle &= \langle f(t), \Psi_{n,m}(t) \rangle - \langle u(t), \Psi_{n,m}(t) \rangle \\ &= \lim_{L \rightarrow \infty} \langle S_{k,M}(t), \Psi_{n,m}(t) \rangle - c_{n,m} \\ &= c_{n,m} - c_{n,m} \\ &= 0. \end{aligned}$$

Therefore $\sum_{m=0}^{2L} \sum_{n=0}^{2^k-1} c_{n,m} \Psi_{n,m}(t)$ converges to $u(t)$ as $L \rightarrow \infty$.

Remark 3.2. *An error bound for the SCWs approximation of a function $u(t) \in L^2[0, 1]$ can be found in [35].*

4. Block-pulse functions

Consider the interval $[0, T)$ and divide it into ω subintervals $[(i-1)h, ih)$, $i = 1, 2, \dots, \omega$ with $h = \frac{T}{\omega}$. Then the block-pulse functions are defined by [36]

$$b_i(t) = \begin{cases} 1, & (i-1)h \leq t < ih, \\ 0, & \text{otherwise.} \end{cases}$$

It is clear from the block-pulse functions' definition that the disjointness property for these functions is satisfied as follows:

$$b_i(t)b_j(t) = \begin{cases} b_i(t), & i = j, \\ 0, & i \neq j, \end{cases} \quad i, j = 1, 2, \dots, \omega.$$

Furthermore, we have the orthogonality property as

$$\int_0^T b_i(t)b_j(t)dt = \begin{cases} h, & i = j, \\ 0, & i \neq j, \end{cases} \quad i, j = 1, 2, \dots, \omega.$$

The block-pulse functions consist a complete orthogonal basis for the space $L^2[0, T)$. Therefore, every real bounded function $u(t)$ which is square integrable on the interval $[0, T)$ can be approximated using the block-pulse functions as

$$u(t) \simeq \sum_{i=1}^{\omega} u_i b_i(t) = U^T B_{\omega}(t), \quad (4.1)$$

where

$$B_{\omega}(t) = [b_1(t), b_2(t), \dots, b_{\omega}(t)]^T,$$

$$U = [u_1, u_2, \dots, u_{\omega}]^T,$$

and

$$u_i = \frac{1}{h} \int_0^t u(t)b_i(t)dt = \frac{1}{h} \int_{(i-1)h}^{ih} u(t)dt.$$

For the block-pulse vector $B_{\omega}(t)$ and the vector U , we have

$$B_{\omega}(t)B_{\omega}^T(t)U \simeq \text{diag}(U)B_{\omega}(t), \quad (4.2)$$

where $\text{diag}(U)$ is the following diagonal matrix

$$\text{diag}(U) = \begin{bmatrix} u_1 & 0 & \dots & 0 \\ 0 & u_2 & \dots & 0 \\ \vdots & \vdots & \ddots & \vdots \\ 0 & 0 & \dots & u_{\omega} \end{bmatrix}.$$

In [36], the authors have introduced the operational matrix of fractional integration of the block-pulse functions. They proved that

$$I^{\alpha} B_{\omega}(t) \simeq F_{\omega \times \omega}^{\alpha} B_{\omega}(t), \quad (4.3)$$

where

$$F_{\omega \times \omega}^{\alpha} = \left(\frac{T}{\omega}\right)^{\alpha} \frac{1}{\Gamma(\alpha+2)} \begin{bmatrix} 1 & \xi_2 & \xi_3 & \xi_4 & \dots & \xi_m \\ 0 & 1 & \xi_2 & \xi_3 & \dots & \xi_{m-1} \\ 0 & 0 & 1 & \xi_2 & \dots & \xi_{m-2} \\ \vdots & \vdots & \ddots & \ddots & \ddots & \vdots \\ 0 & 0 & \dots & 0 & 1 & \xi_2 \\ 0 & 0 & \dots & 0 & 0 & 1 \end{bmatrix}.$$

with $\xi_k = k^{\alpha+1} - 2(k-1)^{\alpha+1} + (k-2)^{\alpha+1}$.

5. Operational matrix of fractional integration

In this section, we introduce the fractional order operational matrix of integration for the GSCWs. To this aim, first we look for a matrix $Q_{\omega \times \omega}$ such that

$$\Psi_{\omega}(t) \simeq Q_{\omega \times \omega} B_{\omega}(t), \tag{5.1}$$

where $\omega = 2^k(2L + 1)$. Using (4.1), we have

$$\Psi_{n,m}(t) = \sum_{i=1}^{\omega} c_i^{n,m} b_i(t),$$

with

$$c_i^{n,m} = \frac{\omega}{T} \int_{\frac{(i-1)T}{\omega}}^{\frac{iT}{\omega}} \Psi_{n,m}(t) dt.$$

Using the definition of the GSCWs, $c_i^{n,m}$ could be nonzero if

$$\frac{n}{2^k} T \leq \frac{i-1}{\omega} T < \frac{i}{\omega} T \leq \frac{n+1}{2^k} T.$$

This implies to have

$$n(2L + 1) + 1 \leq i \leq (n + 1)(2L + 1). \tag{5.2}$$

Taking (4.1) and (5.2) into consideration, we get

$$\Psi_{n,m}(t) = \sum_{i=n(2L+1)+1}^{(n+1)(2L+1)} c_i^{n,m} b_i(t).$$

When $m = 0$, we have

$$c_i^{n,0} = \frac{\omega}{T} \int_{\frac{(i-1)T}{\omega}}^{\frac{iT}{\omega}} \frac{2^{\frac{k}{2}}}{\sqrt{T}} dt = \frac{2^{\frac{k}{2}}}{\sqrt{T}}.$$

For $m = 1, 2, \dots, L$, we obtain

$$\begin{aligned} c_i^{n,m} &= \frac{\omega}{T} \int_{\frac{(i-1)T}{\omega}}^{\frac{iT}{\omega}} \frac{2^{\frac{k+1}{2}}}{\sqrt{T}} \cos\left(\frac{2m\pi}{T}(2^k t - nT)\right) dt \\ &= \frac{2^{\frac{k-1}{2}}(2L+1)}{m\pi\sqrt{T}} \left[\sin\left(2\pi m\left(2^k \frac{i}{\omega} - n\right)\right) - \sin\left(2\pi m\left(2^k \frac{i-1}{\omega} - n\right)\right) \right], \end{aligned}$$

and for $m = L + 1, L + 2, \dots, 2L$, we get

$$\begin{aligned} c_i^{n,m} &= \frac{\omega}{T} \int_{\frac{(i-1)T}{\omega}}^{\frac{iT}{\omega}} \frac{2^{\frac{k+1}{2}}}{\sqrt{T}} \sin\left(\frac{2(m-L)\pi}{T}(2^k t - nT)\right) dt \\ &= \frac{2^{\frac{k-1}{2}}(2L+1)}{(m-L)\pi\sqrt{T}} \left[\cos\left(2\pi(m-L)\left(2^k \frac{i-1}{\omega} - n\right)\right) \right. \\ &\quad \left. - \cos\left(2\pi(m-L)\left(2^k \frac{i}{\omega} - n\right)\right) \right]. \end{aligned}$$

Hence, the matrix $Q_{\omega \times \omega}$ in (5.1) is obtained as

$$Q_{\omega \times \omega} = \begin{bmatrix} Q_0 & O & O & \dots & O \\ O & Q_1 & O & \dots & O \\ O & O & Q_2 & \dots & O \\ \vdots & \vdots & \vdots & \ddots & \vdots \\ O & O & O & \dots & Q_{2^k-1} \end{bmatrix},$$

where O is the zero matrix of dimension $(2L + 1) \times (2L + 1)$ and $Q_n, n = 0, 1, 2, \dots, 2^k - 1$, are $(2L + 1) \times (2L + 1)$ matrices as

$$Q_n = [a_{m,i}^n], \quad m = 0, 1, 2, \dots, 2L, \quad i = 1, 2, 3, \dots, 2L + 1,$$

with $a_{m,i}^n = c_i^{n,m}$.

The matrix $Q_{\omega \times \omega}$ is an invertible matrix, so we have

$$B_{\omega}(t) \simeq Q_{\omega \times \omega}^{-1} \Psi_{\omega}(t). \tag{5.3}$$

Applying the Riemann-Liouville integral operator of order α to (5.1) and then utilizing (4.3) and (5.3), yield

$$I^\alpha \Psi_\omega(t) \simeq Q_{\omega \times \omega} I^\alpha B_\omega(t) \simeq Q_{\omega \times \omega} F_{\omega \times \omega}^\alpha B_\omega(t) \simeq Q_{\omega \times \omega} F_{\omega \times \omega}^\alpha Q^{-1} \Psi_\omega(t).$$

Therefore we have

$$I^\alpha \Psi_\omega(t) \simeq P_{\omega \times \omega}^\alpha \Psi_\omega(t), \quad (5.4)$$

with

$$P_{\omega \times \omega}^\alpha = Q_{\omega \times \omega} F_{\omega \times \omega}^\alpha Q_{\omega \times \omega}^{-1}.$$

In particular, for $T = 1, k = 1, L = 1$ and $\alpha = 0.5$, the GSCWs operational matrix of fractional order integration $P_{\omega \times \omega}^\alpha$ is given by

$$P_{6 \times 6}^{0.5} = \begin{bmatrix} 0.5319 & -0.0253 & -0.2073 & 0.4407 & 0.0218 & 0.0993 \\ -0.0173 & 0.1651 & 0.0991 & 0.0149 & 0.0061 & 0.0148 \\ 0.1418 & -0.0991 & 0.2243 & -0.0679 & -0.0148 & -0.0449 \\ 0. & 0. & 0. & 0.5319 & -0.0253 & -0.2073 \\ 0. & 0. & 0. & -0.0173 & 0.1651 & 0.0991 \\ 0. & 0. & 0. & 0.1418 & -0.0991 & 0.2243 \end{bmatrix}.$$

6. Numerical method

In this section, we use the properties of the GSCWs together with the block-pulse functions to solve a class of nonlinear multi-order FDEs. Consider the following FDE

$$D^\alpha u(t) = \sum_{k=1}^r a_k(t) D^{\beta_k} u(t) + a_0(t) u(t) + a(t) [u(t)]^m + f(t), \quad (6.1)$$

with initial conditions

$$u^{(s)}(0) = u_0^s, \quad s = 0, 1, \dots, [\alpha] - 1,$$

where $\alpha > \beta_1 > \beta_2 > \dots > \beta_r$, D^α denotes the Caputo fractional derivative of order α , $a(t)$, $a_k(t)$, $k = 0, 1, 2, \dots, r$ and $f(t)$ are given known functions, $[\cdot]$ is the ceiling function and $u(t)$ is the unknown function to be determined. In order to obtain a numerical solution for (6.1), we suppose that

$$D^\alpha u(t) \simeq U^T \Psi_\omega(t), \quad (6.2)$$

then using (2.1), (5.4) and (6.2), we have

$$\begin{aligned} u(t) &\simeq U^T P_{\omega \times \omega}^\alpha \Psi_\omega(t) + \sum_{s=0}^{[\alpha]-1} u_0^s \frac{t^s}{s!} \\ &\simeq (U^T P_{\omega \times \omega}^\alpha + U_0^T) \Psi_\omega(t) \\ &= \Lambda_0^T \Psi_\omega(t), \end{aligned} \quad (6.3)$$

where we have used

$$\sum_{s=0}^{[\alpha]-1} u_0^s \frac{t^s}{s!} \simeq U_0^T \Psi_\omega(t),$$

and

$$\Lambda_0 = (U^T P_{\omega \times \omega}^\alpha + U_0^T)^T.$$

Also, taking into consideration (2.2), (5.4) and (6.2), we have

$$D^{\beta_k} u(t) \simeq (U^T P_{\omega \times \omega}^{\alpha - \beta_k} + U_k^T) \Psi_\omega(t) = \Lambda_k^T \Psi_\omega(t), \quad (6.4)$$

where

$$\sum_{s=[\beta_k]}^{[\alpha]-1} u_0^s \frac{t^{s-\beta_k}}{\Gamma(s-\beta_k+1)} \simeq U_k^T \Psi_\omega(t),$$

and

$$\Lambda_k = (U^T P_{\omega \times \omega}^{\alpha - \beta_k} + U_k^T)^T.$$

Now, suppose that

$$\begin{aligned} a_k(t) &\simeq A_k^T \Psi_\omega(t), \quad k = 0, 1, 2, \dots, r, \\ a(t) &\simeq A^T \Psi_\omega(t), \\ f(t) &\simeq F^T \Psi_\omega(t). \end{aligned} \quad (6.5)$$

Substituting approximations (6.3)-(6.5) into (6.1) yields

$$U^T \Psi_\omega(t) = \sum_{k=0}^r A_k^T \Psi_\omega(t) \Psi_\omega^T(t) \Lambda_k + A^T \Psi_\omega(t) \left[\Lambda_0^T \Psi_\omega(t) \right]^m + F^T \Psi_\omega(t). \tag{6.6}$$

By employing (4.2) and (5.1), we get

$$\begin{aligned} A_k^T \Psi_\omega(t) \Psi_\omega^T(t) \Lambda_k &\simeq A_k^T Q_{\omega \times \omega} B_\omega(t) B_\omega^T(t) Q_{\omega \times \omega}^T \Lambda_k \\ &\simeq A_k^T Q_{\omega \times \omega} \text{diag}(Q_{\omega \times \omega}^T \Lambda_k) B_\omega(t) \end{aligned} \tag{6.7}$$

In a similar way, we obtain

$$A^T \Psi_\omega(t) \left[\Lambda_0^T \Psi_\omega(t) \right]^m \simeq A^T Q_{\omega \times \omega} \left[\text{diag}(Q_{\omega \times \omega}^T \Lambda_0) \right]^m B_\omega(t) \tag{6.8}$$

At the end, taking consideration (6.7) and (6.8) into (6.6), we get

$$U^T Q_{\omega \times \omega} - \sum_{k=0}^r A_k^T Q_{\omega \times \omega} \text{diag}(Q_{\omega \times \omega}^T \Lambda_k) - A^T Q_{\omega \times \omega} \left[\text{diag}(Q_{\omega \times \omega}^T \Lambda_0) \right]^m - F^T Q_{\omega \times \omega} = 0,$$

which is a system of nonlinear algebraic equations that can be solved using iterative methods. By solving this system, we obtain the approximate solution $u(t)$ as

$$u(t) \simeq U^T P_{\omega \times \omega}^\alpha \Psi_\omega(t) + \sum_{s=0}^{[\alpha]-1} u_0^s \frac{t^s}{s!}. \tag{6.9}$$

Remark 6.1. In the linear case of the equation (6.1) with constant coefficients, i.e.

$$D^\alpha u(t) = \sum_{k=1}^r a_k D^{\beta_k} u(t) + a_0 u(t) + f(t),$$

the following linear system is resulted from employing our method

$$U^T - \sum_{k=0}^r a_k \Lambda_k^T - a_0 \Lambda_0^T - F^T = 0.$$

7. Illustrative examples

In this section we present four examples and apply the method presented in the previous section for solving them. The function ‘‘FindRoot’’ in ‘‘Mathematica’’ software has been employed for solving the final nonlinear systems obtained by the method.

Example 7.1. Consider the Bagley-Torvik equation [37, 38]

$$aD^2 u(t) = -bD^{3/2} u(t) - cu(t) + c(1+t), \quad t \in [0, 1], \tag{7.1}$$

subject to initial conditions $u(0) = u'(0) = 1$.

The exact solution of this problem is $u(t) = 1 + t$. By considering $k = 0$ and $L = 1$, we employ the present method for this problem with $a = 1, b = 0.5$ and $c = 0.5$. In this case, the basis functions are given by

$$\begin{aligned} \Psi_{0,0}(t) &= \begin{cases} 1, & 0 \leq t < 1, \\ 0, & \text{otherwise,} \end{cases} \\ \Psi_{0,1}(t) &= \begin{cases} \sqrt{2} \cos(2\pi t), & 0 \leq t < 1, \\ 0, & \text{otherwise,} \end{cases} \\ \Psi_{0,2}(t) &= \begin{cases} \sqrt{2} \sin(2\pi t), & 0 \leq t < 1, \\ 0, & \text{otherwise.} \end{cases} \end{aligned}$$

Suppose that

$$D^2 u(t) \simeq u_{0,0} \Psi_{0,0}(t) + u_{0,1} \Psi_{0,1}(t) + u_{0,2} \Psi_{0,2}(t) = U^T \Psi_3(t), \tag{7.2}$$

then using the initial conditions of the problem, we get

$$D^{3/2} u(t) \simeq U^T P_{3 \times 3}^{1/2} \Psi_3(t), \tag{7.3}$$

$$u(t) \simeq U^T P_{3 \times 3}^2 \Psi_3(t) + 1 + t \simeq (U^T P_{3 \times 3}^2 + U_0^T) \Psi_3(t), \tag{7.4}$$

where U_0 is obtained by approximating the function $1 + t$ as

$$U_0 = \left[\frac{3}{2}, 0, -\frac{1}{\sqrt{2}\pi} \right]^T,$$

and $P_{3 \times 3}^{\frac{1}{2}}$ and $P_{3 \times 3}^2$ are given, respectively, by

$$P_{3 \times 3}^{\frac{1}{2}} = \begin{bmatrix} \frac{4}{3\sqrt{\pi}} & \frac{4}{27}(\sqrt{2} + \sqrt{6} - 4)\sqrt{\pi} & \frac{4}{81}(-9\sqrt{2} + 4\sqrt{3} + \sqrt{6})\sqrt{\pi} \\ \frac{\sqrt{2} + \sqrt{6} - 4}{\pi^{3/2}} & \frac{2(-4\sqrt{2} + \sqrt{3} + 5)}{3\sqrt{3}\pi} & \frac{2(8\sqrt{2} - 3\sqrt{3} - 5)}{9\sqrt{\pi}} \\ \frac{9\sqrt{2} - 4\sqrt{3} - \sqrt{6}}{3\pi^{3/2}} & -\frac{2(8\sqrt{2} - 3\sqrt{3} - 5)}{9\sqrt{\pi}} & \frac{2(\sqrt{3} + 4\sqrt{6} - 9)}{9\sqrt{\pi}} \end{bmatrix},$$

$$P_{3 \times 3}^2 = \begin{bmatrix} \frac{1}{6} & \frac{1}{81}\sqrt{\frac{2}{3}}\pi & -\frac{1}{27}(\sqrt{2}\pi) \\ \frac{1}{6\sqrt{6}\pi} & -\frac{1}{54} & 0 \\ \frac{1}{2\sqrt{2}\pi} & 0 & -\frac{5}{54} \end{bmatrix}.$$

By substituting (7.2)–(7.4) into (7.1), we obtain

$$U^T \Psi_3(t) = -0.5U^T P_{3 \times 3}^{\frac{1}{2}} \Psi_3(t) - 0.5(U^T P_{3 \times 3}^2 + U_0^T) \Psi_3(t) + 0.5U_0^T \Psi_3(t),$$

which leads us to have

$$U^T = -0.5U^T P_{3 \times 3}^{\frac{1}{2}} - 0.5U^T P_{3 \times 3}^2.$$

By solving this linear system, the unknown parameters are computed as

$$u_{0,0} = u_{0,1} = u_{0,2} = 0.$$

Thus using (6.9), we get

$$u(t) = 1 + t,$$

which is the exact solution.

Example 7.2. Consider the following multi-order FDE [37, 39]:

$$D^3 u(t) = -D^{5/2} u(t) - [u(t)]^2 + t^4,$$

subject to initial conditions $u(0) = u'(0) = 0$ and $u''(0) = 2$.

The exact solution of this problem is $u(t) = t^2$. The absolute error of the numerical solutions obtained by the present method in this paper is given in Table 1 and Figure 7.1. We have displayed the numerical results for $T = 1$ using the GSCWs with $L = 1$ and $k = 2, 4, 6, 8$ in Table 1. In Figure 7.1, plot of the absolute error obtained by $L = 1$ and different values of k are shown. It is seen from Table 1 and Figure 7.1 that the absolute error decreases as the level of resolution increases.

Table 1: Absolute error at some selected point with $L = 1$ and different values of k for Example 7.2.

t	$k=2$	$k=4$	$k=6$	$k=8$
0.0	2.06×10^{-7}	1.41×10^{-11}	9.22×10^{-16}	5.81×10^{-20}
0.1	3.71×10^{-8}	2.68×10^{-10}	6.23×10^{-12}	4.52×10^{-13}
0.2	3.83×10^{-7}	2.82×10^{-9}	2.26×10^{-10}	1.31×10^{-11}
0.3	8.76×10^{-8}	2.99×10^{-8}	1.51×10^{-9}	9.87×10^{-11}
0.4	3.87×10^{-6}	9.13×10^{-8}	6.63×10^{-9}	3.97×10^{-10}
0.5	2.21×10^{-5}	4.28×10^{-7}	2.06×10^{-8}	1.21×10^{-9}
0.6	9.09×10^{-6}	8.18×10^{-7}	4.54×10^{-8}	2.91×10^{-9}
0.7	3.57×10^{-5}	1.48×10^{-6}	9.99×10^{-8}	6.12×10^{-9}
0.8	3.98×10^{-5}	3.19×10^{-6}	1.85×10^{-7}	1.18×10^{-8}
0.9	1.15×10^{-4}	5.05×10^{-6}	3.38×10^{-7}	2.07×10^{-8}
1.0	9.37×10^{-5}	7.72×10^{-6}	5.35×10^{-7}	3.44×10^{-8}

Example 7.3. Consider the following multi-order FDE [37, 39]:

$$D^4 u(t) = -D^{3.5} u(t) - [u(t)]^3 + t^9,$$

subject to initial conditions $u(0) = u'(0) = u''(0) = 0$ and $u'''(0) = 6$.

The exact solution of this problem is $u(t) = t^3$. The absolute error of the numerical solutions obtained by the present method is given in Table 2 and Figure 7.2. The numerical results for $T = 1$ using the GSCWs with $L = 1$ and $k = 2, 4, 6, 8$ are displayed in Table 2. Plot of the absolute error obtained by $L = 1$ and different values of k are shown in Figure 7.2. The results here confirm the convergence of the numerical solution to the exact solution of this problem.

Example 7.4. As the last example, consider the following linear multi-order FDE [37, 40]:

$$D^2 u(t) = 2Du(t) - D^{0.5} u(t) - u(t) + t^3 - 6t^2 + 6t + \frac{16}{5\sqrt{\pi}} t^{2.5},$$

subject to initial conditions $u(0) = u'(0) = 0$.

The exact solution is $u(t) = t^3$. Numerical results for this example are presented in Table 3 and Figure 7.3. The absolute errors at some selected points on the interval $[0, 1]$ using the GSCWs with $L = 1$ and $k = 2, 4, 6, 8$ are given in Table 3. In Figure 7.3, the exact solution and numerical solution obtained by $L = 1$ and different values of k are displayed. The absolute error reported in Table 3 and Figure 7.3 show the convergence of the numerical solution to the exact solution.

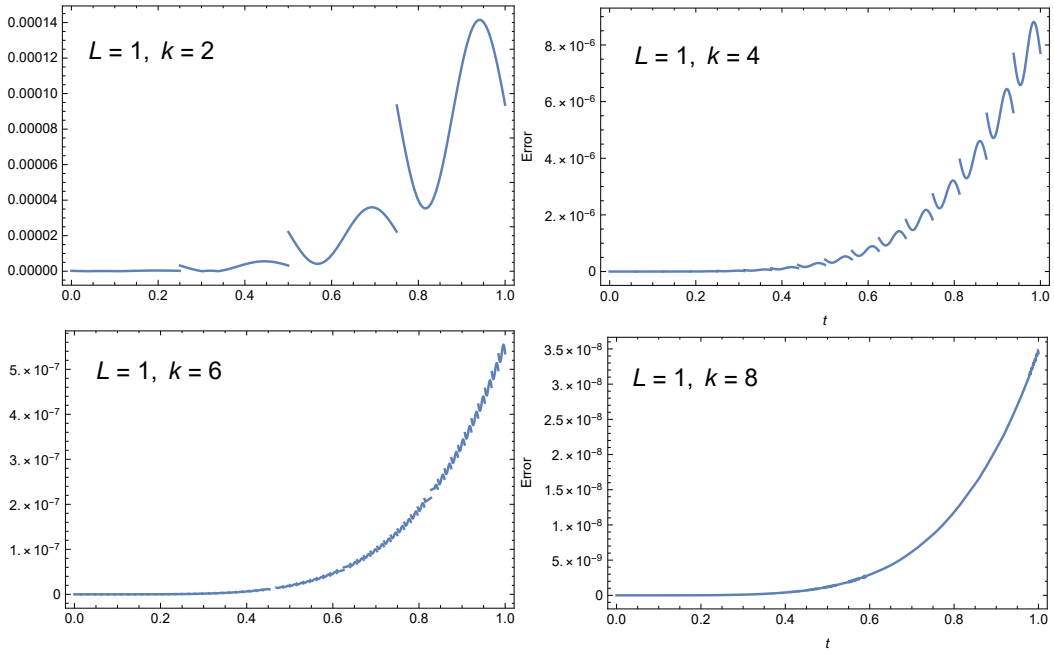


Figure 7.1: Plot of the absolute error with $L = 1$ and $k = 2, 4, 6, 8$ for Example 7.2.

Table 2: Absolute error at some selected point with $L = 1$ and different values of k for Example 7.3.

t	$k=2$	$k=4$	$k=6$	$k=8$
0.0	1.34×10^{-11}	2.22×10^{-19}	3.51×10^{-27}	5.39×10^{-35}
0.1	4.63×10^{-12}	1.03×10^{-16}	2.16×10^{-19}	0.00
0.2	2.31×10^{-11}	8.25×10^{-16}	8.51×10^{-16}	4.51×10^{-17}
0.3	1.88×10^{-9}	1.68×10^{-12}	5.74×10^{-14}	3.94×10^{-15}
0.4	6.26×10^{-9}	1.78×10^{-11}	1.55×10^{-12}	8.80×10^{-14}
0.5	3.06×10^{-7}	6.39×10^{-10}	1.97×10^{-11}	1.07×10^{-12}
0.6	4.30×10^{-8}	2.47×10^{-9}	1.14×10^{-10}	7.58×10^{-12}
0.7	5.27×10^{-7}	9.09×10^{-9}	6.67×10^{-10}	3.98×10^{-11}
0.8	4.17×10^{-8}	5.11×10^{-8}	2.67×10^{-9}	1.73×10^{-10}
0.9	6.36×10^{-6}	1.42×10^{-7}	1.02×10^{-8}	6.16×10^{-10}
1.0	5.66×10^{-5}	3.81×10^{-7}	2.88×10^{-8}	1.91×10^{-9}

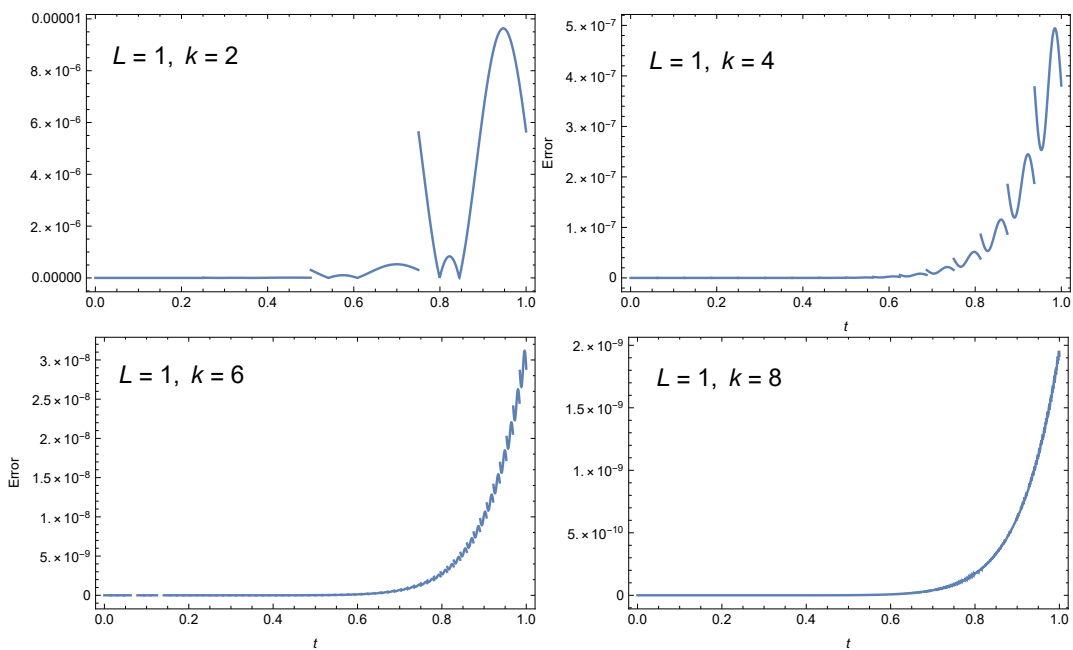
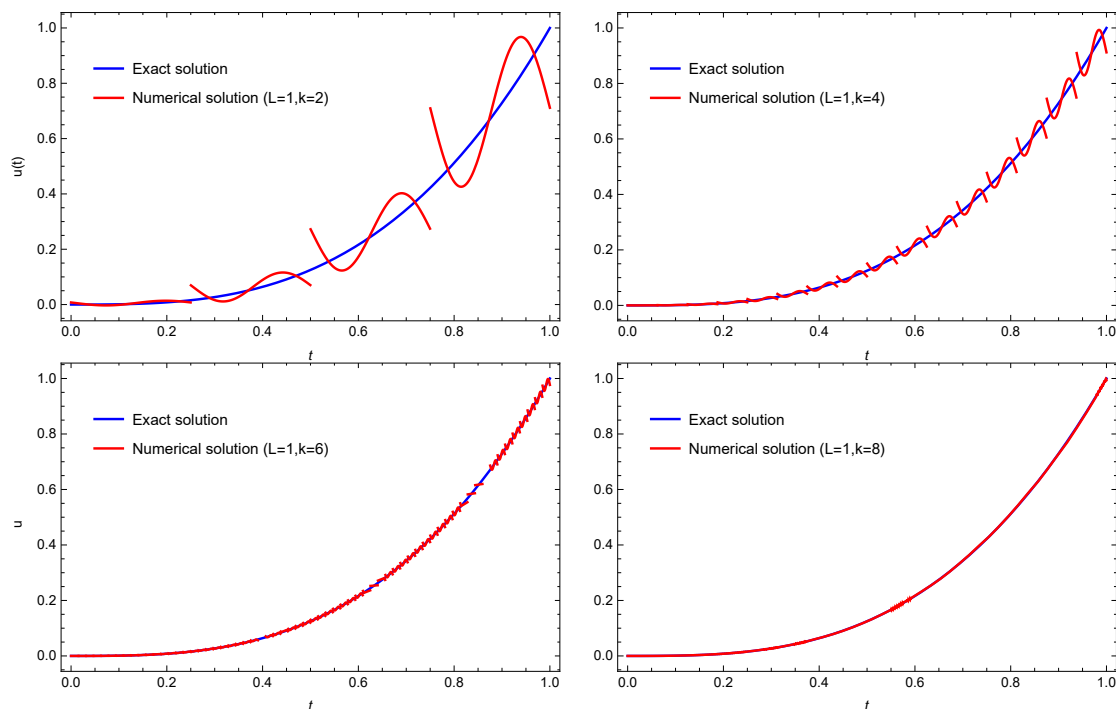


Figure 7.2: Plot of the absolute error with $L = 1$ and $k = 2, 4, 6, 8$ for Example 7.3.

Table 3: Absolute error at some selected point with $L = 1$ and different values of k for Example 7.4.

t	$k=2$	$k=4$	$k=6$	$k=8$
0.0	7.57×10^{-3}	1.17×10^{-4}	1.84×10^{-6}	2.87×10^{-8}
0.1	2.14×10^{-3}	3.84×10^{-4}	7.92×10^{-5}	2.04×10^{-5}
0.2	5.85×10^{-3}	1.08×10^{-3}	2.68×10^{-4}	6.68×10^{-5}
0.3	1.08×10^{-2}	2.45×10^{-3}	6.01×10^{-4}	1.50×10^{-4}
0.4	2.49×10^{-2}	5.04×10^{-3}	1.31×10^{-3}	3.24×10^{-4}
0.5	1.48×10^{-1}	2.64×10^{-2}	6.04×10^{-3}	1.47×10^{-3}
0.6	4.36×10^{-2}	1.20×10^{-2}	2.91×10^{-3}	7.33×10^{-4}
0.7	5.55×10^{-2}	1.30×10^{-2}	3.28×10^{-3}	8.18×10^{-4}
0.8	6.78×10^{-2}	1.72×10^{-2}	4.27×10^{-3}	1.07×10^{-3}
0.9	1.14×10^{-1}	2.58×10^{-2}	6.62×10^{-3}	1.64×10^{-3}
1.0	2.88×10^{-1}	8.79×10^{-2}	2.31×10^{-2}	5.83×10^{-3}

**Figure 7.3:** Plot of the exact solution and numerical solutions with $L = 1$ and $k = 2, 4, 6, 8$ for Example 7.4.

8. Concluding remarks

This work is devoted to the numerical solution of the multi-order fractional differential equations using the generalized sine-cosine wavelets. The fractional order operational matrix of integration has been introduced using the properties of the block-pulse functions and generalized sine-cosine wavelets. Using the properties of sine-cosine wavelets and block-pulse functions, the considered problem is reduced to a system of nonlinear algebraic equations which can be solved using iterative methods. The numerical results of four examples show that the proposed method gives high accuracy approximations of the solutions. As it is seen from the tables and figures, the absolute error decreases as the level of resolution, k , increases.

References

- [1] B. Ross, *The development of fractional calculus 1695–1900*, Hist. Math., **4**(1) (1977), 75–89.
- [2] K. S. Miller, B. Ross, *An Introduction to the fractional calculus and fractional differential equations*, New York, Wiley, 1993.
- [3] K. B. Oldham, J. Spanier, *The fractional calculus*, New York, Academic Press, 1974.
- [4] R. L. Bagley, P. J. Torvik, *Fractional calculus in the transient analysis of viscoelastically damped structures*, AIAA J., **23**(6) (1985), 918–925.
- [5] R. T. Baillie, *Long memory processes and fractional integration in econometrics*, J. Econometr. **73**(1) (1996), 5–59.
- [6] F. Mainardi, *Fractional calculus: some basic problems in continuum and statistical mechanics, fractals and fractional calculus in continuum mechanics*, A. Carpinteri and F. Mainardi, Eds. Vienna, Springer-Verlag, (1997), 291–348.
- [7] Y. A. Rossikhin, M. V. Shitikova, *Applications of fractional calculus to dynamic problems of linear and nonlinear hereditary mechanics of solids*, Appl. Mech. Rev., **50**(1) (1997), 15–67.
- [8] K. B. Oldham, *Fractional differential equations in electrochemistry*, Adv. Eng. Softw., **41**(1) (2010), 9–12.
- [9] V. S. Ertürk, Z. M. Odibat, S. Momani, *An approximate solution of a fractional order differential equation model of human T-cell lymphotropic virus I (HTLV-I) infection of CD4+ T-cells*, Comput. Math. Appl., **62**(3) (2011), 996–1002.
- [10] S. A. El-Wakil, E. M. Abulwafa, E. K. El-Shewy, A. A. Mahmoud, *Ion-acoustic waves in unmagnetized collisionless weakly relativistic plasma of warm-ion and isothermal-electron using time-fractional KdV equation*, Adv. Space Res., **49**(12) (2012), 1721–1727.
- [11] S. Momani, K. Al-Khaled, *Numerical solutions for systems of fractional differential equations by the decomposition method*, Appl. Math. Comput., **162** (2005), 1351–1365.

- [12] Z. M. Odibat, S. Momani, *Application of variational iteration method to nonlinear differential equations of fractional order*, Int. J. Nonlinear Sci. Numer. Simul., **7**(1) (2006), 27–34.
- [13] A. Arikoglu, I. Ozkol, *Solution of fractional integro-differential equations by using fractional differential transform method*, Chaos Solitons Fractals, **40**(2) (2009), 521–529.
- [14] A. Saadatmandi, M. Dehghan, *A new operational matrix for solving fractional order differential equations*, Comput. Math. Appl., **59** (2010), 1326–1336.
- [15] M. Dehghan, J. Manafian, A. Saadatmandi, *Solving nonlinear fractional partial differential equations using the homotopy analysis method*, Numer. Methods Partial Differential Equations, **26** (2010), 448–479.
- [16] Z. Odibat, N. Shawagfeh, *Generalized Taylor's formula*, Appl. Math. Comput., **186** (2007), 286–293.
- [17] Z. Odibat, S. Momani, *Modified homotopy perturbation method: application to quadratic Riccati differential equation of fractional order*, Chaos Solitons Fractals, **36**(1) (2008), 167–174.
- [18] I. Podlubny, *The Laplace transform method for linear differential equations of the fractional order*, 1997, eprint arXiv:func-an/9710005.
- [19] I. Daubechies, *Ten Lectures on Wavelets. CBMS-NFS Series in Applied Mathematics*, SIAM, Philadelphia, PA, 1992.
- [20] I. Daubechies, J. C. Lagarias, *Two-scale difference equations II. local regularity, infinite products of matrices and fractals*, SIAM J. Math. Anal., **23**(4) (1992), 1031–1079.
- [21] S. Mallat, *A theory of multiresolution signal decomposition: the wavelet representation*, IEEE Trans. Pattern Anal. Mach. Intell., **11**(7) (1989), 674–693.
- [22] I. Daubechies, *Orthonormal bases of compactly supported wavelets*, Comm. Pure Appl. Math., **41**(7) (1988), 909–996.
- [23] X. Li, *Numerical solution of fractional differential equations using cubic B-spline wavelet collocation method*, Commun. Nonlinear Sci. Numer. Simul., **17** (2012), 3934–3946.
- [24] Y. M. Chen, M. X. Yi, C. X. Yu, *Error analysis for numerical solution of fractional differential equation by Haar wavelets method*, J. Comput. Sci., **3**(5) (2012), 367–373.
- [25] Y. L. Li, *Solving a nonlinear fractional differential equation using Chebyshev wavelets*, Commun. Nonlinear Sci. Numer. Simul., **15** (2010), 2284–2292.
- [26] H. Jafari, S. A. Yousefi, M. A. Firoozjaee, S. Momani, C.M. Khaliq, *Application of Legendre wavelets for solving fractional differential equations*, Comput. Appl. Math., **62** (2011), 1038–1045.
- [27] P. Rahimkhani, Y. Ordokhani, E. Babolian, *Numerical solution of fractional pantograph differential equations by using generalized fractional-order Bernoulli wavelet*, J. Comput. Appl. Math., **309** (2017), 493–510.
- [28] M. Razzaghi, S. Yousefi, *Sine-cosine wavelets operational matrix of integration and its applications in the calculus of variations*, Int. J. Syst. Sci., **33** (2002), 805–810.
- [29] M. Tavassoli Kajani, M. Ghasemi, E. Babolian, *Numerical solution of linear integro-differential equation by using sine-cosine wavelets*, Appl. Math. Comput., **180** (2006), 569–574.
- [30] M. Ghasemi, E. Babolian, M. Tavassoli Kajani, *Numerical solution of linear Fredholm integral equations using sine-cosine wavelets*, Int. J. Comput. Math., **84** (2007), 979–987.
- [31] N. Irfan, A. H. Siddiqi, *Sine-cosine wavelets approach in numerical evaluation of Hankel transform for seismology*, Appl. Math. Model., **40** (2016), 4900–4907.
- [32] I. Podlubny, *Fractional Differential Equations*, Math. Sci. Eng., **198**, Academic Press, 1999.
- [33] O. Christensen, K. L. Christensen, *Approximation theory: from Taylor polynomial to wavelets*, Birkhauser, Boston, 2004.
- [34] D. Gottlieb, S.A. Orszag, *Numerical analysis of spectral methods*, SIAM, Philadelphia, PA, 1997.
- [35] Y. Wang, T. Yin, L. Zhu, *Sine-cosine wavelet operational matrix of fractional order integration and its applications in solving the fractional order Riccati differential equations*, Adv. Differ. Equ., (2017), 2017: 222.
- [36] A. Kilicman, Z. A. A. Al Zhour, *Kronecker operational matrices for fractional calculus and some applications*, Appl. Math. Comput., **187** (2007), 250–265.
- [37] S. K. Damarla, M. Kundu, *Numerical solution of multi-order fractional differential equations using generalized triangular function operational matrices*, Appl. Math. Comput., **263** (2015), 189 – 203.
- [38] A. E. M. El-Mesiry, A. M. A. El-Sayed, H. A. A. El-Saka, *Numerical methods for multi-term fractional (arbitrary) orders differential equations*, Appl. Math. Comput., **160** (2005), 683–699.
- [39] M. Seifollahi, A. S. Shamloo, *Numerical solution of nonlinear multi-order fractional differential equations by operational matrix of Chebyshev polynomials*, World Appl. Program., **3** (2013), 85–92.
- [40] A. H. Bhrawy, M. M. Tharwat, M.A. Alghamdi, *A new operational matrix of fractional integration for shifted Jacobi polynomials*, Bull. Malays. Math. Sci. Soc., **37** (2014), 983–995.